

**Departures from eustasy in Pliocene sea-level records – Supplementary Information**

Maureen E. Raymo<sup>1\*#</sup>, Jerry X. Mitrovica<sup>2#</sup>, Michael J. O'Leary<sup>3</sup>, Robert M. DeConto<sup>4</sup> and Paul J. Hearty<sup>5</sup>

1. *Department of Earth Sciences, Boston University, 685 Commonwealth Avenue, Boston, MA, USA 02215*

2. *Department of Earth and Planetary Sciences, Harvard University, 20 Oxford Street, Cambridge, MA, USA 02138*

3. *School of Arts and Sciences, University of Notre Dame, Freemantle, WA, Australia 6959*

4. *Department of Geosciences, University of Massachusetts, Amherst, MA, USA 01003*

5. *Department of Environmental Sciences, University of North Carolina, Wilmington, NC, USA 28403.*

*#These authors contributed equally to this work.*

*\*Corresponding author*

**Supplementary Information**

*The sea level equation:* We solve the gravitationally self-consistent sea-level (SL) equation derived in Section 4 and Appendix B2 of Kendall *et al.*<sup>S1</sup> using a pseudo-spectral numerical algorithm with a truncation at spherical harmonic degree and order 256. The algorithm is based on an iterative solver that tracks the gravitationally self-consistent evolution of SL and that is constrained to converge to present-day topography. Within this

solver, perturbations in rotation are computed using a new stability theory<sup>S2</sup> that takes accurate account of the Earth's background oblateness.

*Sensitivity tests:* We first summarize a sequence of numerical SL simulations designed to test the sensitivity of the results presented in the main text to variations in the adopted ice history. Following the general form of the loading implied by the oxygen isotope stack of Lisiecki and Raymo<sup>S3</sup> (see Figure 1), the ice load used in the main text was comprised of two distinct phases. First, the system was assumed to be in isostatic equilibrium until 2.95 Ma. During this period, the ice cover was the same as at present-day, with the exception that the Greenland ice sheet (GIS) and West Antarctic ice sheet (WAIS) had disappeared. At 2.95 Ma, both regions became glaciated to present-day values. From that time to the present, the ice volumes fluctuated with a time history that matched the variation evident in Figure 1. In this period, the ice volumes reached minima that roughly coincided with the present interglacial. The last glacial cycle of the current ice age matched the ICE-5G glaciation history.

In Figure S1 we explore the sensitivity of the predictions to the inclusion of ice volume fluctuations in the pre-2.95 Ma phase of the loading. Specifically, we considered two simulations. In the first, we assumed a simple ramp up in ice volumes at 2.95 Ma. In the second, the WAIS and GIS ice volumes were varied using a single scaling factor between 0 and 1. A scaling of 0 (i.e., an ice-free WAIS and GIS) was adopted at any time in which the oxygen isotope ratio fell to levels at or below the value at the super-interglacial G17 (2.92 per mil). The scaling increased linearly from 0 to a value of 1 (in which case the WAIS and GIS ice volumes were equal to present-day values) at an oxygen isotope ratio of 3.74 per mil (the ratio which defines the local maximum at 3.295 Ma in

Figure 1). The three frames in Figure S1 show the difference between the predicted elevation of paleo-shorelines at the super-interglacials G17, K1 and KM3, respectively, using this modified pre-G17 loading history and the prediction from the first simulation.

It is clear from Figure S1 that the ice and ocean load variation that preceded the G17 super-interglacial perturbs the results by less than  $\sim 1$  m in regions away from the polar ice sheets. We ran a third simulation in which the 0-1 scaling was applied not only to the WAIS and GIS, but also to a northern hemisphere ice cover of amplitude  $\sim 10$  m of equivalent eustatic SL change. In this case, the perturbation to the predictions was of order 2 m. We conclude that any pre-G17 history of loading yields a relatively minor perturbation to the prediction of the total SL elevation map in Figure 2a (or the nearly eustatic far-field elevation in Figure 2b associated with the ramp-up of ice volumes at 2.95 Ma).

In Figure S2 we investigate the origin of the signal in Figure 2c. In particular, we repeat the calculation in this figure with the exception that we zero out the ice and ocean load variation prior to the MIS5e interglacial at 125 ka – the figure shows the difference between this calculation and the result in Figure 2c. The predicted elevation of mid-Pliocene SL markers relative to present is relatively insensitive to pre-MIS5e load history, with the exception of sites near Pleistocene ice sheet centers, and thus we conclude that the results in Figure 2c are dominated by the residual adjustments associated with the last glacial cycle of the ice age.

Our conclusion from this section is that the predicted present-day elevation of mid-Pliocene SL markers in Figure 2a (and also Figure 3a) is: (1) sensitive to the total shift in the baseline interglacial ice volume after the G17 super-interglacial relative to periods

before this, but significantly less sensitive to the details of the pre-G17 loading history; and  
(2) sensitive to only the last glacial cycle of the current ice age.

### References:

- S1. Kendall, R. A., Mitrovica, J. X. & Milne, G. A. On post-glacial sea level: II. Numerical formulation and comparative results on spherically symmetric models. *Geophys. J. Int.* **161**, 679-706 (2005).
- S2. Mitrovica, J. X., Wahr, J., Matsuyama, I. & Paulson, A. The rotational stability of an ice age Earth. *Geophys. J. Int.* **161**, 491-506 (2005).
- S3. Lisiecki, L. E. & Raymo, M. E. A Pliocene-Pleistocene stack of 57 globally distributed benthic  $\delta^{18}\text{O}$  records. *Paleoceanography* 20, PA1003, doi:10.1029/2005PA001153 (2005).

### Supplementary Material Figure Captions:

**S1: Sensitivity of predicted present-day elevation of MPWP SL markers to variations in ice load history prior to 2.95 Ma. a-c.** The difference between the prediction based on a simple ramp up in ice volume at 2.95 Ma and that calculated for the G17 super-interglacial (a), the K1 super-interglacial (b), and the KM3 super-interglacial.

**S2: Sensitivity of the predicted present-day elevation of MPWP SL to ice volume history prior to MIS5e.** The difference between the prediction shown in Figure 2c of the

main text and an analogous prediction in which all ice and ocean load variations prior to the MIS5e interglacial are zeroed out (the figure shows the latter minus the former).

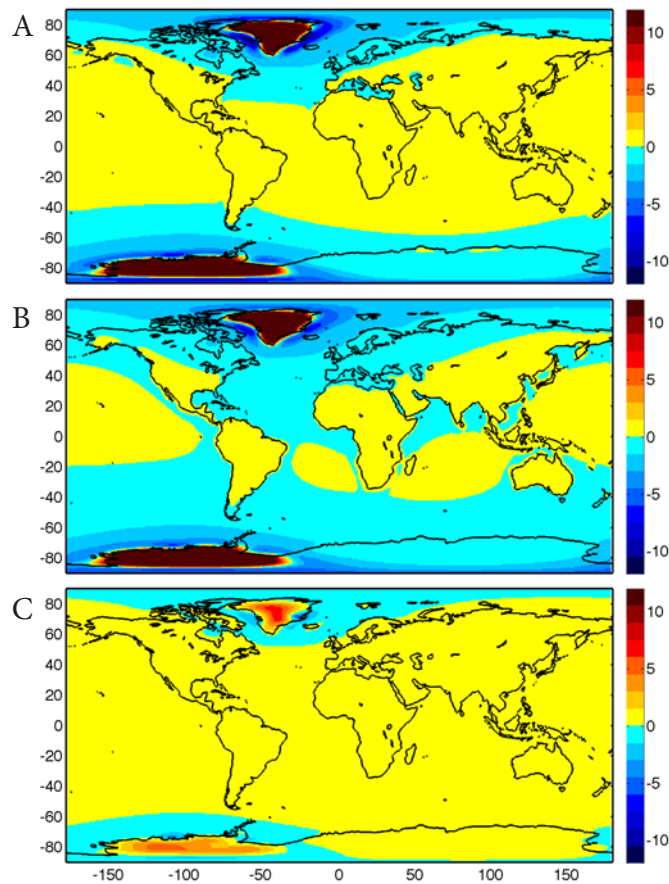


**Figure S1.**

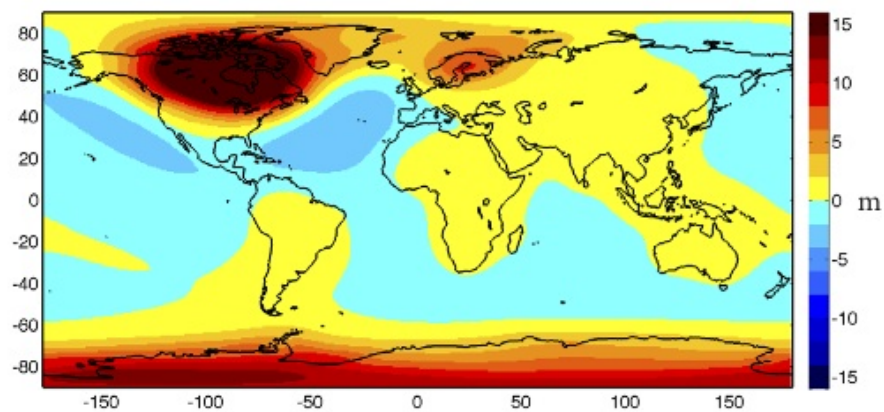


**Figure S2.**